Journal of Cellular Biochemistry 99:1593–1605 (2006)

Caldesmon Is a Cytoskeletal Target for PKC in Endothelium

Natalia V. Bogatcheva, Anna Birukova, Talaibek Borbiev, Irina Kolosova, Feng Liu, Joe G.N. Garcia, and Alexander D. Verin*

Department of Medicine, Section of Pulmonary and Critical Care, The University of Chicago, Chicago, Illinois

Abstract We have previously shown that treatment of bovine endothelial cell (EC) monolayers with phorbol myristate acetate (PMA) leads to the thinning of cortical actin ring and rearrangement of the cytoskeleton into a grid-like structure, concomitant with the loss of endothelial barrier function. In the current work, we focused on caldesmon, a cytoskeletal protein, regulating actomyosin interaction. We hypothesized that protein kinase C (PKC) activation by PMA leads to the changes in caldesmon properties such as phosphorylation and cellular localization. We demonstrate here that PMA induces both myosin and caldesmon redistribution from cortical ring into the grid-like network. However, the initial step of PMA-induced actin and myosin redistribution is not followed by caldesmon redistribution. Co-immunoprecipitation experiments revealed that short-term PMA (5 min) treatment leads to the weakening of caldesmon ability to bind actin and, to the lesser extent, myosin. Prolonged incubation (15–60 min) with PMA, however, strengthens caldesmon complexes with actin and myosin, which correlates with the grid-like actin network formation. PMA stimulation leads to an immediate increase in caldesmon Ser/Thr phosphorylation. This process occurs at sites distinct from the sites specific for ERK1/2 phosphorylation and correlates with caldesmon dissociation from the actomyosin complex. Inhibition of ERK-kinase MEK fails to abolish grid-like structure formation, although reducing PMA-induced weakening of the cortical actin ring, whereas inhibition of PKC reverses PMA-induced cytoskeletal rearrangement. Our results suggest that PKC-dependent phosphorylation of caldesmon is involved in PMA-mediated complex cytoskeletal changes leading to the EC barrier compromise. J. Cell. Biochem. 99: 1593–1605, 2006.

Key words: PKC; caldesmon phosphorylation; cytoskeleton; endothelium

Protein kinase C (PKC) is critically involved in many cellular responses such as cell contraction, migration, proliferation, apoptosis, and secretion [Dempsey et al., 2000]. Phorbol esters, direct and potent PKC activators, are widely employed as useful tools to study PKC function [Siflinger-Birnboim and Johnson, 2003]. However, endothelial responses to phorbol ester-induced PKC activation depend upon the nature of cells and differ significantly from cell to cell type. For example, PMA treatment does not alter monolayer permeability of human umbilical vein EC [Chang et al., 2000], enhances transendothelial resistance of human pulmonary artery EC [Bogatcheva et al., 2003] and results in the loss of endothelial monolayer integrity of bovine pulmonary EC [Verin et al., 2000; Bogatcheva et al., 2003].

Decrease of restrictive barrier function in EC is mainly attributed to the stress fiber formation accompanied by the reduction of junctional integrity [Dudek and Garcia, 2001]. However, phorbol ester-induced decrease in bovine transendothelial resistance was shown to be associated with actin rearrangement into the grid-like structure, different from stress fiber network [Bogatcheva et al., 2003]. The mechanism of PKC-induced cytoskeletal reorganization in bovine EC is not completely understood. The myosin light chain (MLC)

Grant sponsor: NHLBI; Grant numbers: HL 67307, HL 68062, HL 58064, HL 0806675.

*Correspondence to: A.D. Verin, PhD, Department of Medicine, Section of Pulmonary and Critical Care, The University of Chicago, Center for Integrative Science, 929 E. 57th Street, Chicago, Illinois 60637.
E-mail: averin@medicine.bsd.uchicago.edu

Received 13 October 2005; Accepted 21 November 2005
DOI 10.1002/jcb.20823

kinase (MLCK)-independent MLC phosphorylation and concomitant MLC dephosphorylation at MLCK-specific sites seem to cause stress fiber destabilization, which, in turn, leads to the actin rearrangement and bovine EC barrier dysfunction [Bogatcheva et al., 2003]. However, other cytoskeletal targets of PKC or PKC-activated protein kinases could be involved in PMA-induced cytoskeleton remodeling.

In this study, we examined the involvement of myosin- and actin-binding protein caldesmon in PMA-induced cytoskeletal remodeling. We demonstrated that, under PMA challenge, caldesmon undergoes redistribution from cortical ring to a grid-like structure, omitting the initial step of stress fiber formation that is seen in actin and myosin. The formation of grid-like structure is concurrent with the transition of caldesmon, myosin and actin into tight-complex state. Above cytoskeletal rearrangement occurs in co-junction with PMA-mediated caldesmon phosphorylation; ERK1/2, however, seems not to be responsible for the early increase in caldesmon phosphoSer/phosphoThr content. Accordingly, while PKC activation is critical for the PMA-induced actin rearrangement, ERK1/2 activation is not required for the grid-like structure formation. Because of the important role of caldesmon in actomyosin filament organization and stability, we hypothesized that direct or indirect PKC-dependent caldesmon phosphorylation is the causal event, precluding stress fiber disassembly and appearance of the grid-like structure in PMA-treated bovine EC.

MATERIALS AND METHODS

Materials

Protease inhibitor cocktail set III, U0126 and bisindolylmaleimide were purchased from Calbiochem (San Diego, CA). For immunocytochemistry, we used following antibodies: mouse monoclonal antibodies against human L-caldesmon (Transduction Laboratories, Lexington, KY); rabbit polyclonal antiserum against human non-muscle myosin A (heavy chain) (kindly provided by Dr. Adelstein, NIH, Bethesda, MD). Secondary antibody conjugated to immunofluorescent probes (Alexa 488 and 546), Texas-red phalloidin, and Slow Fade Antifade kit were from Molecular probes (Eugene, OR). For immunoprecipitation, we used following antibodies: mouse monoclonal antibodies against human caldesmon or rabbit polyclonal antiserum to caldesmon (Sigma, St. Louis, MO); mouse monoclonal antibody against human alpha-actin (Oncogene Research products, Boston, MA), and rabbit polyclonal myosin antiserum (BTI, Stoughton, MA). Rabbit anti-phosphocaldesmon antisera B1 (Ser^{759}) and B3 (Ser^{789}) were kindly provided by Dr. Adam (Boston Biomedical Research Institute, Watertown, MA). Anti-phosphotyrosine, -phosphoserine, and -phosphothreonine rabbit antibodies were from Zymed Laboratories (South San Francisco, CA).

Cell Culture

Bovine pulmonary artery endothelial cells (BPAEC), line CCL 209, were obtained from American Type Culture Collection (Rockville, MD) at passage 16 and subsequently used at passages 19–21. These cells were cultured in complete media consisting of DMEM supplemented with 20% fetal calf serum, 1% nonessential amino acid solution, 1% antibiotic-antimicotic mixture, and 0.1% endothelial cell growth supplement. Cells were grown to confluency in 75 cm^2 tissue culture flasks and then passaged to the appropriate size cell culture dishes or coverslips in DMEM. For ECIS assay BPAEC were seeded into special culture wells containing vacuum deposited gold filter electrodes. Wells were inoculated at 2×10^4 cells/well. Cells were incubated at 37°C in humidified atmosphere of 5% CO_2/95% air.

Measurement of Transendothelial Electrical Resistance (TER)

TER was measured as we have previously reported [Verin et al., 2000]. In this system, referred as electrical cell-substrate impedance sensing (ECIS), the cells are cultured on the small gold electrode, and culture media serves as electrolyte. The completed electrode array (Applied Biophysics, Troy, NY) was mounted into a holder that made electrical contact through the gold contact pads and was connected to the ECIS instrumentation. In all measurements reported here 1 V and 4 kHz was applied to the sample through 1 MΩ resistor. Cells monolayer resistance data were taken every 0.5 s and processed with Pentium 100 MHz computer, which controlled the output

of amplifier and relay switches to different electrodes.

Localization of F-Actin, Caldesmon, and Myosin in BPAEC

Endothelial cells were grown to subconfluency on gelatinized glass coverslips and treated with protein kinases inhibitors and 100 nM PMA. Cells were fixed in 4% paraformaldehyde for 10 min at room temperature, permeabilized with 0.25% Triton X-100 for 5 min, and blocked with 2% BSA for 30 min. All solutions were prepared in PBS. Incubation with primary antibodies diluted in 2% BSA was performed for 1 h at room temperature. Incubation with Texas Red-phalloidin or with secondary antibody conjugated with fluorescent probe was performed for 1 h at room temperature in the darkness. Coverslips were mounted using Slow Fade Antifade kit (Molecular Probes, Eugine, OR) and analyzed using Nikon Eclipse TE 300 microscope equipped with 20×–100× objective lens.

Cloning of Bovine L-Caldesmon

Reverse transcription-coupled polymerase chain reaction (RT-PCR) was employed to clone caldesmon from endothelium. Total RNA from cultured BPAEC was isolated using silica-gel-based membrane (RNAeasy kit, Qiagen). First-strand cDNA was synthesized from total RNA using both random hexamer and oligo(dT) primers (Advantage RT-for-PCR kit, Clontech). Partial L-caldesmon sequence cloned from bovine epithelium lacking both N- and C-terminal parts was found in GeneBank (Acc. no Z96798). Sense primer for PCR reaction was based on bovine EST sequence (Acc. no BE754254) overlapping with 5′ end of partial bovine caldesmon sequence: 5′-GACATTCTC-TGGTCTCCCTAAATC-3′. To design antisense primer we compared 5′ non-coding regions of L-caldesmon from human (Acc. no D90452), rat (Acc. no U18419) and rabbit (Acc. no L37147). Identical nucleotide stretch was found and the sequence was used as an antisence primer: 5′-TTCACAGCATGGGTTTCTTTAG-3′. PCR amplification was carried out using Advantage 2 Polymerase Mix (Clontech). PCR product was cloned into pCR4-TOPO vector (Invitrogen) and sequenced by Nucleic Acid/Protein Research Core Facility at the Clildren's Hospital of Philadelphia.

Caldesmon Immunoprecipitation Under Nondenaturing Conditions

Confluent BPAEC in 60 mm dishes stimulated with 100 nM PMA for 5–120 min were rinsed with PBS and scraped into 200 μl of immunoprecipitation buffer (10 mM Tris-HCl, pH 7.4, 150 mM NaCl, 1 mM EGTA, 1 mM EDTA, 1% Triton X-100, 0.5% NP-40 supplemented with 0.2 mM $NaVaO_3$, 20 mM NaF, and protease inhibitors cocktail set III (Calbiochem)). Cell suspension was aspirated five times through the needle of tuberculin syringe and cenrifuged at 10,000*g* for 5 min at 4°C. Supernatant was precleared with 15 μl of protein G-sepharose suspension (Amersham Pharmacia Biotech, Inc, Piscataway, NJ), incubated with 2 μl of anti-caldesmon mouse monoclonal antibody for 1 h with agitation and then with protein G-sepharose for additional 1 h. Immunocomplex was harvested by centrifugation, washed three times with IP buffer, resuspended in SDS sample buffer and analyzed by Western blotting using anti-caldesmon, anti-actin, and anti-myosin antibodies. All experiments were repeated at least three times.

Detection of PKC Translocation

Differential detergent fractionation of EC was performed as described [Liu et al., 2002]. Briefly, endothelial monolayers were incubated with cytosol extraction buffer (0.01% digitonin, 10 mM PIPES, pH 6.8, 300 mM sucrose, 100 mM NaCl, 3 mM $MgCl_2$, 5 mM EDTA, 5 μM phallacidin, protease inhibitor cocktail set III 1:200) with agitation for 10 min on ice. The digitonin-soluble fractions were collected by aspiration; the residual material was incubated with membrane extraction buffer (0.5% Triton X-100, 10 mM PIPES, pH 7.4, 300 mM sucrose, 100 mM NaCl, 3 mM EDTA, 5 μM phallacidin, and protease inhibitor cocktail set III 1:200) with agitation for 20 min on ice. The Triton-soluble fractions were collected by aspiration; both digitonin-soluble (cytosolic) and Triton-soluble (membrane) fractions were analyzed by Western immunoblotting using anti-PKC alpha specific monoclonal antibody from Santa-Cruz Biotechnology (Santa Cruz, CA).

Caldesmon Phosphorylation Assay

Confluent BPAEC monolayers in 35 mm dishes were treated with 100 nM PMA for specified time periods, then rinsed twice with

PBS and scraped into immunoprecipitation buffer (see above). Caldesmon immunoprecipitates were prepared and processed as described before. Phosphoserine, phosphothreonine, and phosphotyrosine content was assessed by probing nitrocellulose membranes with antiphosphoserine, phosphothreonine, and phosphotyrosine antibodies. All experiments were repeated at least two times.

Phosphorylation of caldesmon by proline-directed protein kinases in total cell lyzates was analyzed using anti-phosphocaldesmon antisera kindly provided by Dr. Adam. These antisera recognize serine residues (Ser^{759} and Ser^{789} in human h-caldesmon sequence) phosphorylated by ERK1/2 or p38 in mammalian caldesmon [D'Angelo et al., 1999]. All experiments were repeated at least three times.

Determination of Rac GTPase Activity

Endothelial cells grown in 100 mm dishes were incubated with agonists in serum-free M199 medium. Cells were scraped into 500 μl immunoprecipitation buffer (see above) and homogenized by pipetting. After a brief centrifugation, 300 μl of supernatants were incubated with 10 μg of human p21-binding domain of PAK1 (residues 67–150), conjugated with agarose (Upstate Biotechnology, Lake Placid, NY) for 30 min. The agarose beads were washed with the immunoprecipitation buffer and resuspended in 30 μl of SDS-containing buffer. The precipitates as well as initial homogenates were subjected to electrophoresis in 15% SDS–PAGE; anti-Rac monoclonal antibody was used to compare the level of activated Rac (immunoprecipitates) with the total Rac (initial homogenates).

RESULTS

Involvement of Actin Cytoskeleton in PMA-Mediated EC Barrier Dysfunction

PMA is known to increase permeability across the monolayer of BPAEC [Stasek et al., 1992; Verin et al., 2000]. To establish the role of actin cytoskeleton in PMA-induced barrier dysfunction, we monitored the changes in BPAEC monolayer integrity after PMA treatment in the presence or absence of F-actin stabilizer, phalloidin. Previously, phalloidin was successfully used for stabilization of actin filaments in intact endothelium [Alexander et al., 1988]. BPAEC grown on the gold microelectrode reveal a steady state electrical resistance (approx. 1,000 Ω) characteristic for the confluent cell monolayer. PMA treatment results in the time-dependent decline in electrical resistance (Fig. 1). The effect of PMA started within 5 min with maximal decrease in resistance achieved after 30 min of exposure. This barrier reducing response was sustained for 2–3 h. Pretreatment of endothelial cells with phalloidin did not have noteworthy effect on the resistance of unstimulated monolayer but significantly attenuated PMA-mediated decline in TER.

PKC-Induced Alterations in Localization and Distribution of Cytoskeletal Proteins Actin, Myosin, and Caldesmon

To directly monitor PMA-induced changes in actin organization we used fluorescence microscopy of Texas Red phalloidin-stained cells. In quiescent subconfluent cells the vast majority of F-actin localizes in the close vicinity to the plasma membrane, forming a thick cortical ring. Incubation with PMA for as short as 5 min significantly thins the cortical actin in EC and induces moderate stress fiber formation (Fig. 2A). In contrast, longer incubation (15 min and more) with PMA leads to the complete substitution of stress fibers with the novel type

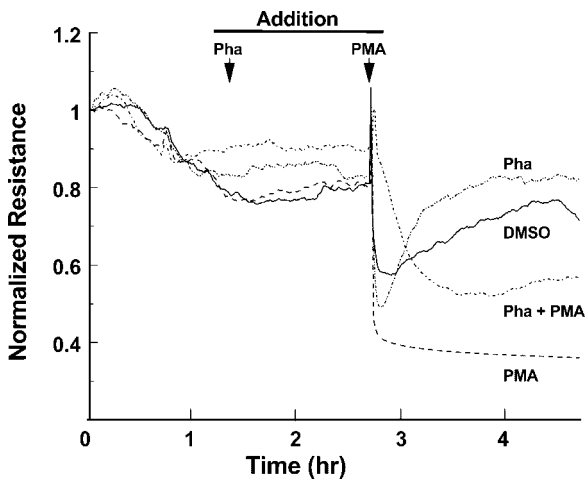

Fig. 1. Stabilization of the actin cytoskeleton by phalloidin attenuates PMA-induced increase in transendothelial electrical resistance. Endothelial cell monolayer resistance was monitored for 5 h. At time 0, cells were rinsed with serum-free media and incubated for approximately 1 h to monitor basal electrical resistance. EC were pretreated with phalloidin (1 μM) or vehicle (EtOH) for 1.5 h and then challenged with either 100 nM PMA or vehicle (0.1% DMSO). Shown are the results from the representative experiments (n = 4).

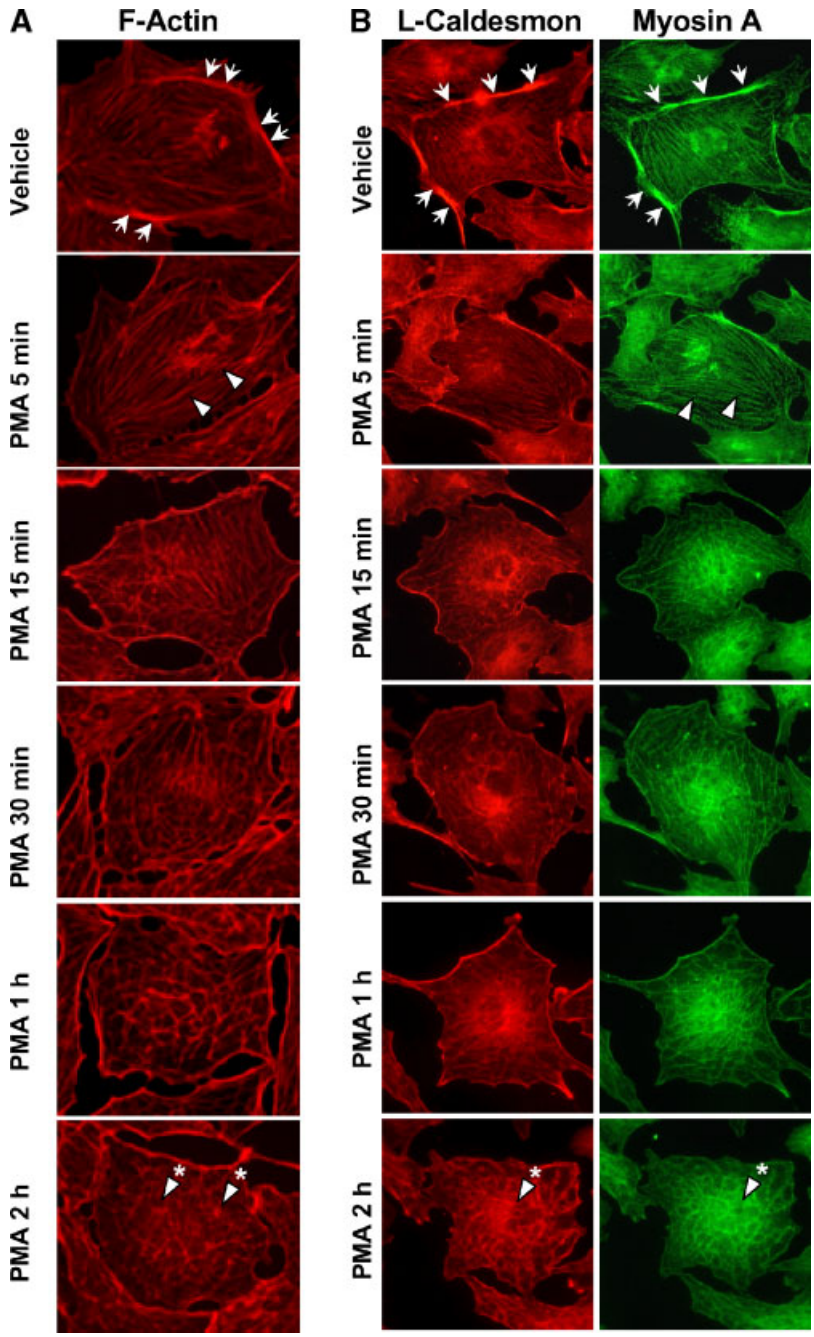

Fig. 2. Effect of PMA on actin (**A**), caldesmon, and myosin (**B**) localization in BPAEC. Shown are immunofluorescent images (magnification 60×) of subconfluent BPAEC, challenged with 100 nM PMA for the indicated time periods, fixed and stained with Texas Red-phalloidin (A) or double stained with an anti-caldesmon and anti-myosin antibodies (B) as described in METHODS. Bovine EC demonstrated PMA-induced actin and myosin rearrangement with rapid disintegration of cortical ring (arrows) and moderate stress fiber induction (block arrows), followed by the reduction of stress fibers and complete reorganization of cytoskeletal proteins into grid-like structures (block arrows with asterisks). Caldesmon, initially co-localized with the cortical ring, is not incorporated into stress fibers. However, later it participates in the formation of the grid-like structure. [Color figure can be viewed in the online issue, which is available at www.interscience.wiley.com.]

of actin network with grid-like distribution. This grid-like actin structure persists for as long as 2 h (Fig. 2A). To address the composition of the cytoskeleton during PMA-induced rearrangement, we detected actin-binding proteins localization in PMA-treated BPAEC. Double immunofluorescent staining with anti-caldesmon and anti-myosin antibodies revealed

that myosin follows the same complex redistribution in PMA-challenged EC (Fig. 2B). Myosin filaments located under the membrane tend to thin after 5 min of stimulation but those crossing the middle of cell undergo moderate induction. Antibody to caldesmon, however, reveals no increase in caldesmon-containing filamentous structures after first 5 min of incubation with PMA. Later both caldesmon and myosin reorganize into grid-like filamentous network localized in the middle of the cells.

Bovine L-Caldesmon Structure Analysis

We have cloned bovine endothelial L-caldesmon (GeneBank accession numbers AY154474 and AAN46421). Bovine and human caldesmons share greater than 90% identity at the amino acid level. However, several non-conservative point substitutions are presented in the

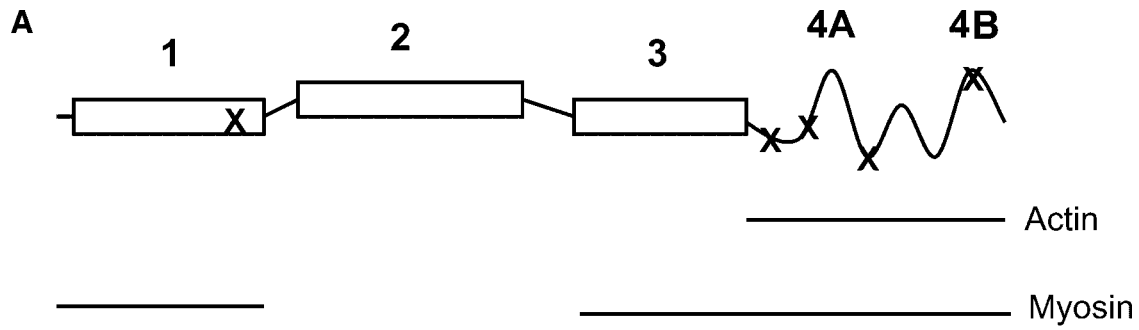

B

```
Human CaD     MDDFERRRELRRQKREEMRLEAERIAYQRNDDDEEEAARERRRRARQERLRQKQEEESLG 60
Bovine CaD    MDDFERRRELRRQKREEMRLEAERIAYQRNDDDEEEAARERRRRARQERLRQKQEEEALG 60
                                                                        :
Human CaD     QVTDQVEVNAQNSVPDEEAKTTTTNTQVEGDDEAAFLERLARREERRQKRLQEALERQKE 120
Bovine CaD    QVTDQVEVNTQNSVPDEEVKTTTTNTQAEGDDEAALLERLARREERRQKRLQEALERQKE 120
                    :         .         .         :
Human CaD     FDPTITDASLSLPSRRMQNDTAENETTEKEEKSESRQERYEIEETETVTKSYQKNDWRDA 180
Bovine CaD    FDPTITDASLSLSSRRMQNDTTDNETAEKEGRSESRQERQELEETEIVTKSHQKNDWMEA 180
                         .         ::    :   *:       * :    *    :     *:
Human CaD     EENKKEDKEKEEEEEEKPKRGSIGENQIKDEKIKKDKEPKEEVKSFMDRKKGFTEVKSQN 240
Bovine CaD    EEKKKEEKEKEEEEEEKPKPGSIEENQLKDEKTKKDKESKD-VKRFLDAKKGFTEVKSQN 239
                :   :              *   *    :    *      . :    * : *
Human CaD     GEFMTHKLKHTENTFSRPGGRASVDTKEAEGAPQVEAGKRLEELRRRRGETESEEFEKLK 300
Bovine CaD    GEFMTHKLKHAENTFSRAGGRVS-EAKEAEGTSQVEAGKRLEELRRRRGETESEEFEKLK 298
                         :       .    .   ::      :.
Human CaD     QKQQEAALELEELKKKREERRKVLEEEEQRRKQEEADRKLREEEEKRRLKEEIERRRAEA 360
Bovine CaD    QKQQEAALELEELKKKREERRKVLEEEEQRKKQEEAERKVREEEEKRRLKEEIERRRAEA 358
                                                :      :   :
Human CaD     AEKRQKMPEDGLSDDKKPFKCFTPKGSSLKIEERAEFLNKSVQKSSGVKSTHQAAIVSKI 420
Bovine CaD    AEKRQKMPEDGLSEDKKPFKCFTPKGSSLKIEERAEFLNKSVQKS-GVKPTHQAAVVSKI 417
                          :                                          .     :
Human CaD     DSRLEQYTSAIEGTKSAKPTKPAASDLPVPAEGVRNIKSMWEKGNVFSSPTAAGTPNKET 480
Bovine CaD    DSRLEQYTSAIEGTKAAKPTKPAASDLPVPAEGVRNIKSMWEKGNVFSSPTASGTPNKET 477
                          :                                          :
Human CaD     AGLKVGVSSRINEWLTKTPDGNKSPAPKPSDLRPGDVSSKRNLWEKQSVDKVTSPTKV   538
Bovine CaD    AGLKVGVSSRINEWLTKTPEGSKSPAPKPSDLRPGDVSGKRNLWEKQSVDKVTSPTKV   535
                                  : .                 .
```

Fig. 3. Sequence comparisons of human and bovine L-caldesmon. **A**: The four-domain model of h-caldesmon proposed by Marston and Redwood [1991]. N-terminal domain, containing about 210 residues, interacts with myosin, tropomyosin, and, possibly, calmodulin. Second domain of ~250 residues, absent in L-caldesmon, is able to bind tropomyosin. Third domain (~180 residues) interacts with myosin, tropomyosin, and actin. C-terminal domain (~120 residues) with complex tertiary structure provides myosin, tropomyosin, actin, and calmodulin binding [Mezgueldi et al., 1994; Huber et al., 1995, 1996; Vorotnikov et al., 1997; Gusev, 2001]. Asterisks mark the putative phosphorylation sites by protein kinase C [Vorotnikov et al., 1994]. **B**: Amino acid alignment of human L-caldesmon (Acc. no AAA58420), and bovine L-caldesmon (Acc. No AAN 46421). Shown are non-conservative substitutions (different physico-chemical characteristics (asterisks)), conservative substitutions (similar physico-chemical characteristics (colons)), and semi-conservative substitutions (intermingled physico-chemical characteristics (dots)). Myosin-binding regions are underlined with solid line; high-affinity actin-binding region is underlined with dashed line.

N-terminal myosin-binding and C-terminal myosin- and actin-binding domains (Fig. 3). Of particular interest could be two Pro/Ala and Pro/Ser substitutions and singular amino acid deletion in the 3d, tropomyosin-binding domain of caldesmon. Besides, myosin-binding site located in the C-terminus of the 3D domain also contains Ser/Pro substitution, possibly affecting secondary structure and binding properties of the domain.

Effect of PMA on the Complex Formation Between Caldesmon, Actin, and Myosin

To analyze caldesmon association with actin and myosin in PMA-challenged cells, we immunoprecipitated protein complexes with anti-caldesmon antibody under non-denaturing conditions. We observed, that short-term incubation with PMA decreased the amount of actin and myosin in caldesmon immunoprecipitates indicating weakening of caldesmon/actomyosin intraction. Longer incubation with PMA, however, led to the dramatic induction of the caldesmon-actin and caldesmon-myosin complex formation (Fig. 4).

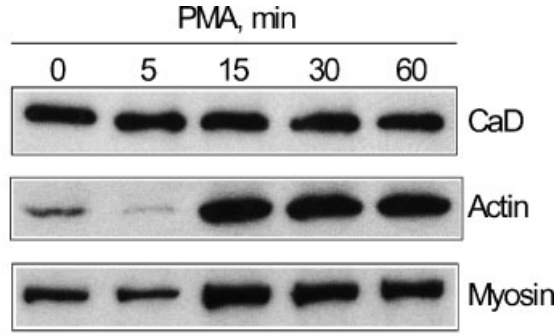

	0min	5min	15min	30min	60min
CD	1 ±0.00	1.12 ±0.27	1.08 ±0.27	1.16 ±0.14	1.25 ±0.11
Actin	1 ±0.00	0.37 * ±0.11	4.78 * ±1.00	4.71* ±1.62	5.19 * ±2.31
Myosin	1 ±0.00	0.87 ±0.15	1.57 * ±0.42	1.21 ±0.19	1.10 ±0.25

Fig. 4. PMA affects the binding of caldesmon to myosin and actin in bovine EC. Confluent BPAEC were treated with 100 nM PMA or vehicle (0.1% DMSO) for the time indicated, extracted with Triton/NP-containing buffer and subjected to immunoprecipitation with anti-caldesmon antibody. The presence of caldesmon, actin, and myosin in immunoprecipitates was analyzed with specific antibodies. Images were quantified with ImageQuant 5.2 Software and presented as mean ± SE. Significant changes in actin and myosin content with $P < 0.05$ are marked with asterisks. PMA induces early caldesmon dissociation from the complex with actin and myosin, followed by the reassociation of actin, caldesmon and myosin into novel tightly bound ensemble.

Caldesmon Phosphorylation in PMA-Treated Bovine EC

To reveal the mechanism of myosin-caldesmon-actin complexes rearrangement we analyzed caldesmon phosphorylation in PMA-stimulated BPAEC. Here we demonstrate that translocation and activation of PKC (Fig. 5A,B) is quickly followed by the increase in caldesmon phosphorylation, with phospho-Ser and phospho-Thr incorporation reaching maximum at 5 and 10 min of incubation, respectively. However, while PKC stays associated with membrane until 30 min of incubation, phospho-Thr content declines after 10 min. No changes in caldesmon phospho-Tyr level were detected (data not shown).

Adam et al. [1992] demonstrated that a central role in agonist-dependent caldesmon phosphorylation belongs to ERK1/2, the mitogen-activated kinase. As rapid and sustained ERK1/2 activation was shown earlier in PMA-treated BPAEC [Verin et al., 2000], we assessed proline-directed caldesmon phosphorylation using phospho-specific antibodies towards phospho-Ser^{759} and Ser^{789}. Immunostaining with phospho-Ser^{759}-specific antiserum did not reveal any signal in control or PMA-treated cells (data not shown). The level of Ser^{789} phosphorylation reached the maximum after 30 min of exposure to PMA and persisted for at least 2 h (Fig. 6). Western immunoblotting with phospho-ERK1/2 antibody demonstrated that ERK1/2 activation occurs after 5 min of PMA exposure, much earlier, than caldesmon Ser^{789} phosphorylation reaches detectable level. Taken together, these data raise the possibility that some other kinase, different from ERK1/2, is responsible for early caldesmon phosphorylation in PMA-treated cells. Among the kinases, known to phosphorylate caldesmon, are p21-activated kinase PAK, CaM kinase II, and PKC [Sutherland and Walsh, 1989; Tanaka et al., 1990; Foster et al., 2000].

Analysis of Rac GTPase Activity and CaM Kinase II Autophosphorylation Level in PMA-Induced EC

Previous studies have implicated PAK in caldesmon phosphorylation in smooth muscle

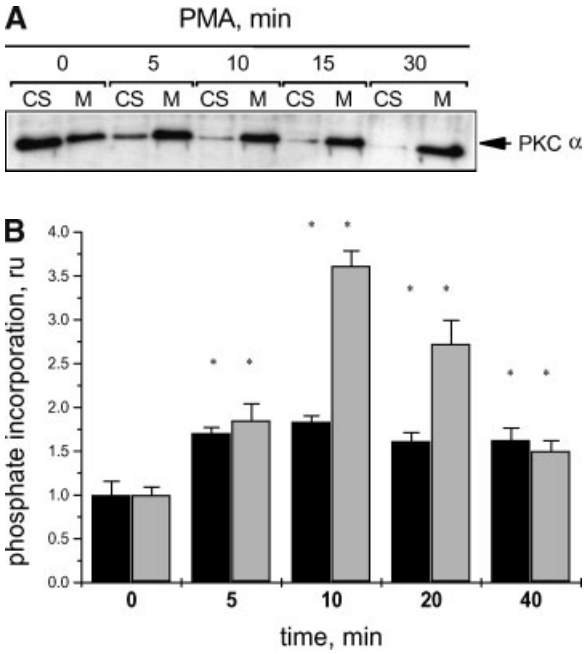

Fig. 5. Effect of phorbol 12-myristate 13-acetate (PMA) on PKC translocation and caldesmon phosphorylation. **A**: PKC alpha immunoblots of 100 nM PMA-treated endothelial cell subcellular fractions obtained by differential detergent fractionation as described in Materials and Methods. PKC alpha immunoreactivity was completely translocated from the cytosolic to membrane fraction, reflecting PKC activation. **B**: The time course of caldesmon phosphorylation on serine and threonine in PMA-treated EC. Confluent BPAEC were challenged with PMA or vehicle (0.1% DMSO) for the time indicated and then immunoprecipitated with anti-caldesmon antibody. Immunoprecipitates were analyzed using western blotting with anti-phosphoserine and anti-phosphothreonine antibodies. Images were quantified with ImageQuant 5.2 Software and presented as mean ± SE. Phosphoserine (black) and phosphothreonine (grey) content was assessed as ratio to the control values (no stimulation). Significant changes in phosphoserine and phosphothreonine content with $P < 0.05$ are marked with asterisks.

cells [Van Eyk et al., 1998]. Since PAK could be readily activated by the small G-protein Rac, and activation of Rac2 was shown in PMA-treated neutrophils [Akasaki et al., 1999], we checked the possibility that Rac became induced in BPAEC during PMA treatment. The method we used utilizes co-immunoprecipitation of activated Rac with PAK-1 p21-binding domain (PBD), attached to the agarose beads. We found that 10 min challenge with PMA fails to increase the level of Rac in PAK-1 PBD precipitates, whereas 1 min sphingosine-1-phosphate treatment (positive control) significantly activates Rac and promotes its interaction with PAK-1 (Fig. 7).

We also considered possible involvement of CaM kinase II into early caldesmon phosphorylation, since this kinase is able to phosphorylate caldesmon in vitro [Ikebe and Reardon, 1990] and was shown to participate in phorbol ester-induced mouse oocyte activation [Inagaki et al., 1997]. A possible mechanism of phorbol ester-dependent activation of CaM kinase II in the absence of calcium influx likely involves increased availability of calmodulin due to the massive phosphorylation of PKC substrates [Hulvershorn et al., 2001]. We assessed the level of CaM kinase II autophosphorylation, indicative of calcium-independent enzyme activity, in PMA-treated bovine endothelial cells (ECs). We failed to detect any increase in the level of CaM kinase II autophosphorylation during 5–120 min PMA stimulation (data not shown), suggesting the absence of CaM kinase activation and CaMK-dependent caldesmon phosphorylation in PMA-treated EC.

Effect of PKC and ERK1/2 Inhibition on F-Actin Rearrangement in PMA-Treated Endothelium

Earlier we have shown that both PKC and ERK1/2 inhibition attenuates PMA-induced endothelial barrier dysfunction in BPAEC monolayer [Verin et al., 2000]. To examine the requirement of PKC and ERK1/2 for PMA-induced actin reorganization, we pretreated BPAEC with PKC inhibitor bisindolylmaleimide and MEK inhibitor U0126. Incubation with pharmacologic inhibitors of PKC and MEK did not affect significantly BPAEC cytoskeleton in the absence of phorbol ester. Pretreatment with bisindolylmaleimide completely abolished PMA-induced grid-like structure formation and partly inhibited cortical actin disappearance (Fig. 8). Preincubation with U0126, however, failed to block the rearrangement of actin into the grid-like structure, nevertheless preventing the weakening of cortical ring. The ultimate outcome of these data is that PKC and ERK1/2 seem to control cytoskeleton in different cellular compartments of PMA-stimulated BPAEC.

DISCUSSION

PKC functions as central intracellular signal amplifier for various extracellular agonists. Similar to the natural activator of PKC diacylglycerol, phorbol esters were shown to induce the conformational changes in PKC structure leading to the intramolecular Zn^{2+} release and PKC activation [Korichneva et al., 2002]. This

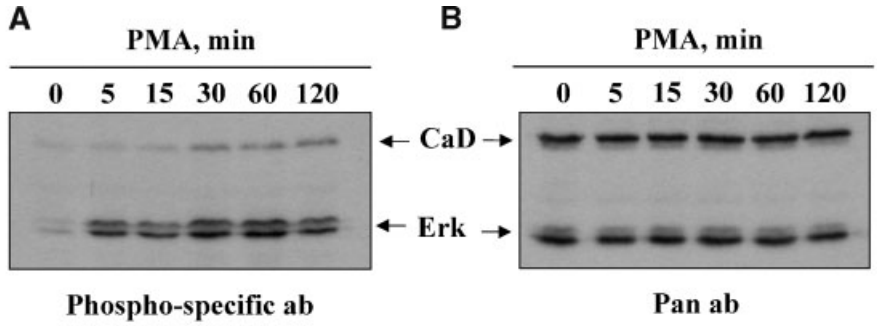

	Phospo-specific ab						Pan ab					
	0 min	5 min	15 min	30 min	60 min	120 min	0 min	5 min	15 min	30 min	60 min	120 min
CD	1.00 ± 0.56	0.75 ± 0.37	2.53* ±0.23	12.8 * ±1.24	18.8 * ±6.94	19.2 * ±3.98	1.00 ±0.03	0.90 ±0.01	0.85 ±0.01	0.86 ±0.07	0.94 ±0.05	1.00 ±0.05
Erk	1.00 ±0.03	4.23 * ±0.04	3.78* ±0.37	3.55* ±0.17	3.49* ±0.63	4.54* ±0.37	1.00 ±0.04	0.98 ±0.03	0.91 ±0.06	1.02 ±0.02	1.02 ±0.01	1.07 ±0.08

Fig. 6. ERK1/2 activation and ERK-specific caldesmon phosphorylation in PMA-treated bovine EC. Confluent BPAEC were challenged with 100 nM PMA for the time indicated. Caldesmon phosphorylation was analyzed by Western immunoblotting with endothelial cell homogenates with anti-caldesmon antibodies specific to the phospho-Ser 789 (number corresponds to the residue in the structure of human h-caldesmon). The level of ERK activation was analyzed with anti-phospho-ERK antibody. Equal loading was verified using anti-caldesmon and anti-panERK antibodies. Images were quantified with ImageQuant 5.2 Software and presented as mean of normalized values ± SE. Significant changes in phospho-ERK and phosphocaldesmon content with $P < 0.05$ are marked with asterisks.

makes phorbol esters a valuable tool to study the physiological effects of PKC activation in many tissues and cell types.

Phorbol esters are known to increase significantly endothelial cell permeability. The mechanism involves rearrangement of actomyosin cytoskeleton without a rise in intracellular calcium or MLCK activation [Patterson et al., 1994; Garcia et al., 1995; Bogatcheva et al., 2003]. To determine the role of actin reorganization in PMA-induced endothelial barrier dysfunction, we inhibited filament remodeling with F-actin stabilizer phalloidin. Our data (Fig. 1) indicate that PMA-induced actin rearrangement is apparently critical for the barrier compromise in bovine endothelium since phalloidin significantly attenuates the response of EC to PMA. The incomplete effect of phalloidin may be associated with the restricted ability of this compound to permeate intact cells.

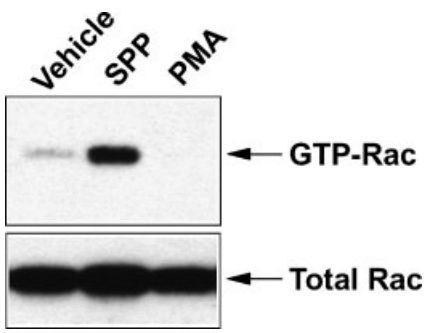

Fig. 7. PMA does not activate Rac in bovine pulmonary EC. BPAEC were incubated for 1 min with sphingosine-1-phosphate (1 μM) as positive control and PMA (100 nM) for 10 min. The activated GTP-bound Rac was precipitated from cell lysates by agarose-conjugated human PAK-1 p21-binding domain and immunoblotted by anti-Rac monoclonal antibody. Total Rac content was detected using original cell lysates. The results indicate rapid spingosine-1-phosphate-, but not PMA-induced Rac activation.

Phorbol esters were shown to exert diverse effects on actin cytoskeleton depending on the cell type used in the study and the conditions of cell culturing. Although in many cells phorbol ester increases F-actin content [Downey et al., 1992; Masson-Gadais et al., 1997; Vaaraniemi et al., 1999], PMA-induced depolymerization of actin network was also shown [Vaaraniemi et al., 1999]. Earlier we demonstrated that PMA stimulates biphasic remodeling of the actin cytoskeleton in subconfluent ECs. The process includes transient and moderate microfilament formation, followed by the rearrangement of actin network into grid-like structure [Bogatcheva et al., 2003]. Here we show that

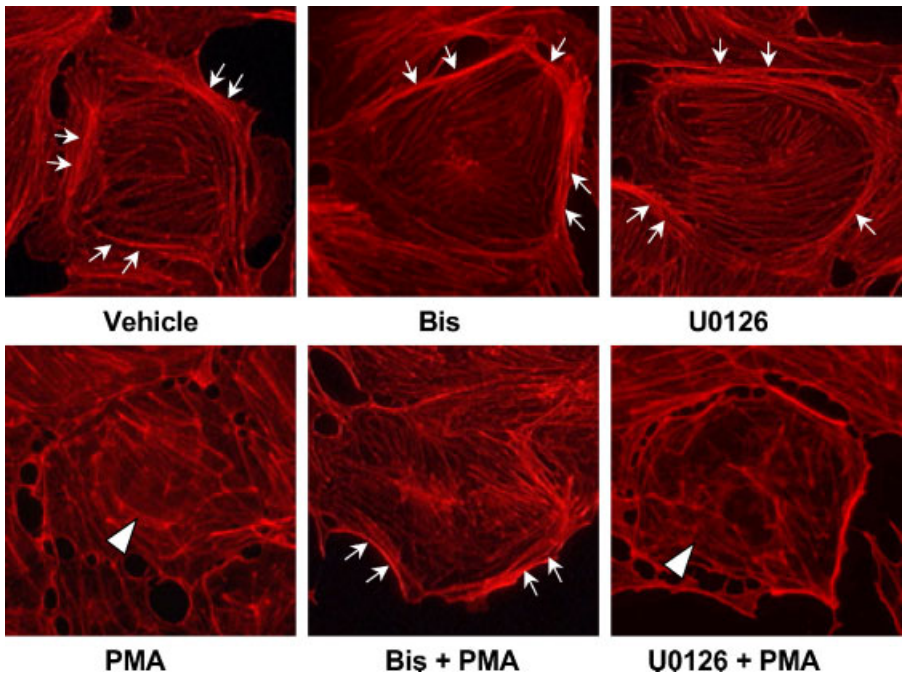

Fig. 8. The effect of PKC and ERK1/2 inhibition on PMA-induced actin rearrangement in bovine EC. Shown are immunofluorescent images (magnification 60×) of subconfluent BPAEC, preincubated for 60 min with either 1 μM PKC inhibitor bisindolylmaleimide (Bis) or 5 μM MEK inhibitor U0126, and challenged with PMA for 60 min. Pretreatment with BIM significantly diminishes thinning of cortical actin ring (arrows) and formation of grid-like structure (block arrows), whereas pretreatment with U0126 blocks the cortical ring dissipation only. [Color figure can be viewed in the online issue, which is available at www.interscience.wiley.com.]

myosin undergoes similar redistribution in PMA-treated BPAEC (Fig. 2), with initial localization along induced stress fibers and subsequent reorganization into the grid-like filamentous network. Our results are consistent with the observation of other authors that PMA induces two-step redistribution of actin and myosin in BPAEC [Zhao and Davis, 1999]. We hypothesized earlier that transition of actin and myosin from stress fibers to the grid-like complex is caused by the dephosphorylation of MLC at MLCK-specific sites, leading to the filament destabilization [Bogatcheva et al., 2003]. The focus of this study was attributed to the caldesmon, as this protein was shown to stabilize filaments of dephosphorylated smooth muscle myosin under physiological conditions [Katayama et al., 1995]. We have demonstrated that caldesmon, localized together with actin and myosin at the cortical ring of resting cells, does not appear as a part of spanning cell stress fibers during the first phase of PMA-induced cytoskeletal rearrangement (5 min of treatment). Later on, however, caldesmon is readily localized with grid-like structure composed of actin and myosin.

Caldesmon appears to play the crucial role in the regulation of actomyosin interaction and the organization of actomyosin cytoskeleton [Mornet et al., 1988; Huber et al., 1995, 1996; Lamb et al., 1996; Goncharova et al., 2001]. Although the majority of studies were done using smooth-muscle protein, our recent work proves that non-muscle caldesmon regulates the cytoskeletal organization and cell motility similar to smooth muscle caldesmon [Mirzapoiazova et al., 2005]. Here, we show that caldesmon is likely involved in the PMA-induced cytoskeletal reorganization in EC, as its properties readily change under PMA stimulation. During the first 5 min, caldesmon significantly loses the ability to bind actin and, to the lesser extent, myosin. Such dissociation of caldesmon from the actomyosin complex may be a prerequisite of the filaments destabilization necessary for the cytoskeletal transition to the novel state. Longer stimulation with PMA leads to re-association of caldesmon with actin and myosin.

The initial increase of overall caldesmon phosphorylation is of particular importance (Fig. 5), as it correlates with the changes in actin- and myosin-binding properties of

caldesmon (Fig. 4) and precedes the reorganization of actin cytoskeleton into grid-like structure (Fig. 2). We show here, that despite the immediate activation of ERK1/2 by PMA, early (5 min) caldesmon phosphorylation is unlikely to be mediated by this enzyme (Figs. 5,6). Correspondingly, Krymsky et al. [1999] demonstrated that early caldesmon phosphorylation in phorbol ester-treated smooth muscle cells was driven by protein kinase distinct from ERK1/2. It was observed earlier, that activation of PKC is associated with transient recruitment of cytosolic MAP kinase to the surface membrane followed by later redistribution of this enzyme toward contractile filaments [Khalil and Morgan, 1993]. This could explain the delay between ERK1/2 activation and ERK-specific caldesmon phosphorylation in smooth muscle and endothelial cells.

Apparently, at least three other protein kinases should be considered as main candidates on the role of caldesmon kinases during EC response to PMA. One of them is PKC, which is directly activated by phorbol ester and able to phosphorylate caldesmon [Vorotnikov et al., 1994; Verin et al., 2000]. Two other caldesmon kinases, Rac-dependent PAK and calcium/calmodulin-dependent protein kinase II, could be involved in caldesmon phosphorylation in PMA-treated EC, as in some cell types phorbol ester was shown to activate Rac or increase free calmodulin concentration [Inagaki et al., 1997; Akasaki et al., 1999]. Our results revealed that both PAK and CaM kinase II are not activated in PMA-treated BPAEC. Therefore PKC seems the most plausible candidate due to its early and robust activation by phorbol ester. PKC was reported to incorporate phosphate into multiple Ser/Thr residues located within myosin- actin- and tropomyosin-binding sites of caldesmon [Vorotnikov et al., 1994]. Phosphorylation affects the ability of caldesmon to interact with actin-tropomyosin and to inhibit myosin ATPase [Vorotnikov et al., 1994]. Application of constitutively active PKCε to permeabilized smooth muscle cells affected the contraction, suggesting a possible physiological role of caldesmon phosphorylation by PKC [Horowitz et al., 1996].

Our data demonstrate that pharmacological inhibition of PKC completely abrogates PMA-induced cytoskeleton rearrangement in bovine EC. In contrast, ERK1/2 inhibition attenuates the cortical ring dissociation, but fails to prevent the grid-like structure formation in PMA-stimulated EC. These data are consistent with the different impact of PKC and ERK inhibition onto PMA-induced barrier dysfunction in bovine endothelial monolayer [Verin et al., 2000]. As we had shown, bisindolylmaleimide diminishes PMA-induced changes in TER more effectively than PD-98059 or olomoucin [Verin et al., 2000]. Taken together, our results support the previous finding, that cortical ring weakening along with rearrangement of stress fibers into the grid-like structure represents the cytoskeletal basis of PMA-induced bovine endothelium barrier dysfunction. Thus, in contrast to permeability changes, induced by thrombin, PMA-induced permeability increase is not associated with stress fiber formation and contraction. Further studies are needed to characterize the role of grid-like structure formation in PMA-induced barrier dysfunction.

We speculate that the mechanism of PMA-induced BPAEC cytoskeletal rearrangement is as follows. Early PKC-dependent caldesmon phosphorylation affects actin- and myosin-binding properties of caldesmon, leading to the caldesmon dissociation from actomyosin complex. While PMA-induced decrease of Ser^{19}/Thr^{18} MLC phosphorylation leads to the stress fibers destabilization [Bogatcheva et al., 2003], the absence of the stabilizing effect of caldesmon facilitates the disassembly of actomyosin filaments. Stress fibers rearrange into the grid-like structure, which recruits caldesmon to form novel tightly cross-linked complexes.

We have shown earlier that PMA-induced formation of grid-like actomyosin structures is characteristic for BPAEC, as opposed to HPAEC [Bogatcheva et al., 2003]. We hypothesized that such cytoskeletal rearrangement is linked to the loss of barrier function, since HPAEC do not exhibit reduction of transendothelial resistance under PMA treatment. We do not know if the nature of endothelial caldesmon contributes to the differences in HPAEC and BPAEC cytoskeleatal rearrangements. We have found several non-conservative substitutions in the structure of bovine L-caldesmon, however, future research will be required to reveal the possible effect of these substitutions on the caldesmon function.

In conclusion, we have characterized PMA-induced cytoskeletal rearrangement in bovine EC and have linked it with the alteration in

actin-caldesmon-myosin complex composition. PMA rapidly increases the level of caldesmon phosphorylation, however, activation of ERK does not contribute to the overall caldesmon phosphorylation until the late phase of response to PMA. Early caldesmon phosphorylation, presumably directly by PKC, causes caldesmon dissociation from actomyosin filaments. After cytoskeleton rearrangement into the grid-like network, caldesmon re-associates with actin and myosin to form tight complexes persisting during the later phase of response to PMA. This process precedes ERK-specific phosphorylation of caldesmon. The results of this study represent the potential mechanism by which phorbol ester might alter cytoskeleton organization and barrier function of endothelium.

ACKNOWLEDGMENTS

This work was supported by grants HL 67307, HL 68062 and HL0806675 (A.D.V.); HL 58064 (J.G.N.G.), from the National Heart, Lung and Blood Institute. The authors gratefully acknowledge Lakshmi Natarajan, Nurgul Moldabaeva, and Dylan Burdette for superb technical assistance. We also thank Dr. R.S. Adelshtein and Dr. L.P. Adam for their generous supply of specific antibodies.

REFERENCES

Adam LP, Gapinski CJ, Hathaway DR. 1992. Phosphorylation sequences in h-caldesmon from phorbol ester-stimulated canine aortas. FEBS Lett 302:223–226.

Akasaki T, Koga H, Sumimoto H. 1999. Phosphoinositide 3-kinase-dependent and -independent activation of the small GTPase Rac2 in human neutrophils. J Biol Chem 274:18055–18059.

Alexander JS, Hechtman HB, Shepro D. 1988. Phalloidin enhances endothelial barrier function and reduces inflammatory permeability in vitro. Microvas Res 35: 308–315.

Bogatcheva NV, Verin AD, Wang P, Birukova AA, Birukov KG, Mirzopoyazova T, Adyshev DM, Chiang ET, Crow MT, Garcia JG. 2003. Phorbol esters increase MLC phosphorylation and actin remodeling in bovine lung endothelium without increased contraction. Am J Physiol 285:L415–L426.

Chang YS, Munn LL, Hillsley MV, Dull RO, Yuan J, Lakshminarayanan S, Gardner TW, Jain RK, Tarbell JM. 2000. Effect of vascular endothelial growth factor on cultured endothelial cell monolayer transport properties. Microvasc Res 59:265–277.

D'Angelo G, Graceffa P, Wang CA, Wrangle J, Adam LP. 1999. Mammal-specific, ERK-dependent, caldesmon phosphorylation in smooth muscle. Quantitation using novel anti-phosphopeptide antibodies. J Biol Chem 274: 30115–30121.

Dempsey EC, Newton AC, Mochly-Rosen D, Fields AP, Reyland ME, Insel PA, Messing RO. 2000. Protein kinase C isozymes and the regulation of diverse cell responses. Am J Physiol 279:L429–L438.

Downey GP, Chan CK, Lea P, Takai A, Grinstein S. 1992. Phorbol ester-induced actin assembly in neutrophils: Role of protein kinase C. J Cell Biol 116:695–706.

Dudek SM, Garcia JG. 2001. Cytoskeletal regulation of pulmonary vascular permeability. J Appl Physiol 91: 1487–1500.

Foster DB, Shen LH, Kelly J, Thibault P, Van Eyk JE, Mak AS. 2000. Phosphorylation of caldesmon by p21-activated kinase. Implications for the Ca(2+) sensitivity of smooth muscle contraction. J Biol Chem 275:1959–1965.

Garcia JG, Davis HW, Patterson CE. 1995. Regulation of endothelial cell myosin light chain phosphorylation. J Cell Physiol 163:510–522.

Goncharova EA, Shirinsky VP, Shevelev AY, Marston SB, Vorotnikov AV. 2001. Actomyosin cross-linking by caldesmon in non-muscle cells. FEBS Lett 497:113–117.

Gusev NB. 2001. Some properties of caldesmon and calponin and the participation of these proteins in regulation of smooth muscle contraction and cytoskeleton formation. Biochemistry (Mosc) 66:1112–1121.

Horowitz A, Clement-Chomienne O, Walsh MP, Morgan KG. 1996. Epsilon-isoenzyme of protein kinase C induces a Ca(2+)-independent contraction in vascular smooth muscle. Am J Physiol 271:C589–C594.

Huber PA, Fraser ID, Marston SB. 1995. Location of smooth-muscle myosin and tropomyosin binding sites in the C-terminal 288 residues of human caldesmon. Biochem J 312:617–625.

Huber PA, El-Mezgueldi M, Grabarek Z, Slatter DA, Levine BA, Marston SB. 1996. Multiple-sited interaction of caldesmon with Ca(2+)-calmodulin. Biochem J 316: 413–420.

Hulvershorn J, Gallant C, Wang CA, Dessy C, Morgan KG. 2001. Calmodulin levels are dynamically regulated in living vascular smooth muscle cells. Am J Physiol 280: H1422–H1426.

Ikebe M, Reardon S. 1990. Phosphorylation of smooth muscle caldesmon by calmodulin-dependent protein kinase II. Identification of the phosphorylation sites. J Biol Chem 265:17607–17612.

Inagaki N, Suzuki S, Kitai H, Nakatogawa N, Kuji N, Iwahashi K, Yoshimura Y. 1997. Effect of KN-62, a selective inhibitor of calmodulin-dependent kinase II, on mouse oocyte activation. J Assist Reprod Genet 14:609–616.

Katayama E, Scott-Woo G, Ikebe M. 1995. Effect of caldesmon on the assembly of smooth muscle myosin. J Biol Chem 270:3919–3925.

Khalil RA, Morgan KG. 1993. PKC-mediated redistribution of mitogen-activated protein kinase during smooth muscle cell activation. Am J Physiol 265:C406–C411.

Korichneva I, Hoyos B, Chua R, Levi E, Hammerling U. 2002. Zinc release from protein kinase C as the common event during activation by lipid second messenger or reactive oxigen. J Biol Chem 277:44327–44331.

Krymsky MA, Chibalina MV, Shirinsky VP, Marston SB, Vorotnikov AV. 1999. Evidence against the regulation of caldesmon inhibitory activity by p42/p44erk mitogen-activated protein kinase in vitro and demonstration of another caldesmon kinase in intact gizzard smooth muscle. FEBS Lett 452:254–258.

Lamb NJ, Fernandez A, Mezgueldi M, Labbe JP, Kassab R, Fattoum A. 1996. Disruption of the actin cytoskeleton in living nonmuscle cells by microinjection of antibodies to domain-3 of caldesmon. Eur J Cell Biol 69:36–44.

Liu F, Schaphorst KL, Verin AD, Jacobs K, Birukova A, Day RM, Bogatcheva N, Bottaro DP, Garcia JG. 2002. Hepatocyte growth factor enhances endothelial cell barrier function and cortical cytoskeletal rearrangement: Potential role of glycogen synthase kinase-3beta. FASEB J 16:950–962.

Marston SB, Redwood CS. 1991. The molecular anatomy of caldesmon. Biochem J 279:1–16.

Masson-Gadais B, Salers P, Bongrand P, Lissitzky JC. 1997. PKC regulation of microfilament network organization in keratinocytes defined by a pharmacological study with PKC activators and inhibitors. Exp Cell Res 236:238–247.

Mezgueldi M, Derancourt J, Calas B, Kassab R, Fattoum A. 1994. Precise identification of the regulatory F-actin- and calmodulin-binding sequences in the 10-kDa carboxyl-terminal domain of caldesmon. J Biol Chem 269:12824–12832.

Mirzapoiazova T, Kolosova IA, Romer L, Garcia JG, Verin AD. 2005. The role of caldesmon in the regulation of endothelial cytoskeleton and migration. J Cell Physiol 203:520–528.

Mornet D, Harricane MC, Audemard E. 1988. A 35-kilodalton fragment from gizzard smooth muscle caldesmon that induces F-actin bundles. Biochem Biophys Res Commun 155:808–815.

Patterson CE, Davis H, Schaphorst K, Garcia JG. 1994. Mechanism of cholera toxin prevention of thrombin- and PMA-induced endothelial cell barrier dysfunction. Microvasc Res 48:212–235.

Siflinger-Birnboim A, Johnson A. 2003. Protein kinase C modulates pulmonary endothelial permeability: A paradigm for acute lung injury. Am J Physiol 284:L435–L451.

Stasek JE Jr, Patterson CE, Garcia JG. 1992. Protein kinase C phosphorylates caldesmon77 and vimentin and enhances albumin permeability across cultured bovine pulmonary artery endothelial cell monolayers. J Cell Physiol 153:62–75.

Sutherland C, Walsh MP. 1989. Phosphorylation of caldesmon prevents its interaction with smooth muscle myosin. J Biol Chem 264:578–583.

Tanaka T, Ohta H, Kanda K, Hidaka H, Sobue K. 1990. Phosphorylation of high-Mr caldesmon by protein kinase C modulates the regulatory function of this protein on the interaction between actin and myosin. Eur J Biochem 188:495–500.

Vaaraniemi J, Palovuori R, Lehto VP, Eskelinen S. 1999. Translocation of MARCKS and reorganization of the cytoskeleton by PMA correlates with the ion selectivity, the confluence, and transformation state of kidney epithelial cell lines. J Cell Physiol 181:83–95.

Van Eyk JE, Arrell DK, Foster DB, Strauss JD, Heinonen TY, Furmaniak-Kazmierczak E, Cote GP, Mak AS. 1998. Different molecular mechanisms for Rho family GTPase-dependent, Ca^{2+}-independent contraction of smooth muscle. J Biol Chem 273:23433–23439.

Verin AD, Liu F, Bogatcheva N, Borbiev T, Hershenson MB, Wang P, Garcia JG. 2000. Role of ras-dependent ERK activation in phorbol ester-induced endothelial cell barrier dysfunction. Am J Physiol 279:L360–L370.

Vorotnikov AV, Gusev NB, Hua S, Collins JH, Redwood CS, Marston SB. 1994. Phosphorylation of aorta caldesmon by endogenous proteolytic fragments of protein kinase C. J Muscle Res Cell Motil 15:37–48.

Vorotnikov AV, Marston SB, Huber PA. 1997. Location and functional characterization of myosin contact sites in smooth muscle caldesmon. Biochem J 328:211–218.

Zhao Y, Davis HW. 1999. Signaling pathways in thrombin-induced actin reorganization in pulmonary artery endothelial cells. Exp Lung Res 25:23–39.